Article

UDC 536.24; 004.94

https://doi.org/10.31489/2025PH3/68-76

Received: 28.04.2025
Accepted: 07.06.2025

A.S. Zhumanbayeva, N.Zh. Jaichibekov✉, D.Y. Kurmanova

L.N. Gumilyov Eurasian National University, Astana, Kazakhstan

Study of the Influence of Turbulence Models on Hydrodynamic and Thermal Parameters of Heat Carriers in Calculations of Heat Exchangers

In this paper, the heat exchange processes between a cold (oil) and a highly heated (water) heat carrier in a “tube-in-tube” type heat exchanger with a parallel flow scheme are studied using semi-empirical turbulence models: k-ω SST, k-ε, and Transition SST. The analysis of the obtained results showed that the *k*-ω SST turbulence model was more preferable for the calculation of a heat exchanger with a sufficiently small tube diameter, because of the effect of the boundary layer in the tube. This turbulence model more pronouncedly reproduces the laminar-turbulent transition, which is carried out in these processes, where the viscosity of oil strongly depends on temperature. Finite difference and finite volume methods were chosen for numerical modelling and calculation of heat exchange processes. The calculations were carried out on the basis of Computational Fluid Dynamics, using the Ansys Fluent. The RANS equations closed by means of the gamma-Retheta turbulence model, which takes into account the laminar-turbulent transition and the k-ω SST model equations, were used for numerical modelling of coolant hydrodynamics. Based on the proposed turbulence model, the distributions of hydrodynamic and thermal parameters and similarity criteria (Re, Pr, Nu) of the process along the length of the tube are obtained.

Keywords: heat transfer, numerical calculation, heat exchanger, oil, hydrodynamics, cooling fluids, heat flow, laminar-turbulent transition, intermittency, heat exchange intensity, viscosity

✉*Corresponding author*: Jaichibekov, Nurbolat, jaich@mail.ru

Introduction

Fluid dynamics in the innertube space of a heat exchanger is defined by the process’s complexity and is determined by numerous parameters. Research in works [1, 2] focus on numerical modeling of heat exchange in different types of HE. The findings of heat exchanger calculations are utilized to optimize and intensify heat exchange processes [3–5]. In particular, it has been demonstrated that when turbulence develops, the influence of injected oil viscosity on the hydraulic resistance of the pipeline is greatly reduced.

Unsteady three-dimensional Navier-Stokes equations expressed regarding instantaneous (direct numerical modelling), average (solution of Reynolds equations), or space-filtered (modeling of massive vortices) functions explain the unsteady spatial flow of a viscous incompressible fluid. To close the averaged Reynolds or filtered Navier-Stokes equations, the eddy viscosity hypothesis is used.

Works in [6–9] investigate the accuracy of various turbulence models used to close the Reynolds equations. A comparison of the accuracy of various turbulence models used to close the Reynolds equations is the subject of further research. Basically, the available calculations use the $k-\varepsilon$, $k-\omega$ SST (Shear Stress

Transport) and Transition SST models. The calculations make it possible to achieve a satisfactory agreement between the results of numerical modeling and the data from industrial experiments. At the same time, the calculations performed using two-parameter turbulence models do not take into account the laminar-turbulent transition, which affects the determination of the effective length of the HE [10–13].

This paper presents the results of numerical calculations using various turbulence models: the $k-\varepsilon$ model, including models, that take into account the laminar-turbulent transition ($k-\omega$ SST, Transition SST). The calculation results are compared with the results of the distribution of the average mass temperature of oil and water (cold and hot coolants) along the length of the heat exchanger [10], obtained using the Log-Mean Temperature Difference (LMTD) method and they are consistent with the literature data [14; p. 4.1]. A comparative analysis of the obtained results based on these models with data from a physical experiment and calculations based on semi-empirical dependencies allows us to select an effective turbulence model for use in calculations of direct-flow HE.

Calculation method

Numerical modelling of heat transfer processes was based on finite difference and finite volume methods. To solve this problem, computational fluid dynamics (CFD) methods were used using the Ansys Fluent software package, which allows taking into account the effects of turbulence and heat transfer in fluid flows. The use of CFD methods in the design of HE allows not only to improve the main indicators of their performance while ensuring acceptable mechanical reliability, but also to create designs that practically do not need modification. Thermal and hydrodynamic calculations make it possible to analyze temperature distribution in various conditions of heat exchange with diffusion and convection processes, to optimize the geometry of heat exchangers and to calculate hydraulic resistances.

Closing equations for determining turbulent viscosity, which is calculated using the kinetic energy of turbulence, the dissipation of turbulence energy, and the intermittency parameter for the above turbulence models, are commonly used in computational fluid dynamics and in various engineering and scientific applications. These equations for the above three models are given below. All empirical coefficients used in these equations are defined in [13].

$k-\varepsilon$ *model*: the turbulence kinetic energy k and the dissipation energy of turbulence ε are determined from the following system of equations (1):

$$\begin{gathered}\frac{\partial}{\partial t}(\rho k)+\frac{\partial}{\partial x_i}(\rho k u_i)=\frac{\partial}{\partial x_j}\left[\left(\mu+\frac{\mu_t}{\sigma_k}\right)\frac{\partial k}{\partial x_j}\right]+G_k+G_b-\rho\varepsilon-Y_M+S_k\\ \frac{\partial}{\partial t}(\rho\varepsilon)+\frac{\partial}{\partial x_i}(\rho\varepsilon u_i)=\frac{\partial}{\partial x_j}\left[\left(\mu+\frac{\mu_t}{\sigma_\varepsilon}\right)\frac{\partial \varepsilon}{\partial x_j}\right]+C_{1\varepsilon}\frac{\varepsilon}{k}(G_k+C_{3\varepsilon}G_b)-C_{2\varepsilon}\rho\frac{\varepsilon^2}{k}+S_\varepsilon\end{gathered}\tag{1}$$

$k-\omega$ *SST (Shear Stress Transport) model* (2):

$$\begin{gathered}v_j\frac{\partial \mathrm{Re}_{\theta t}}{\partial x_j}=P_{\theta t}+\frac{\partial}{\partial x_j}\left[\sigma_{\theta t}(\nu+\nu_t)\frac{\partial \mathrm{Re}_{\theta t}}{\partial x_j}\right],\\ v_j\frac{\partial\gamma}{\partial x_j}=P_\gamma-E_\gamma+\frac{\partial}{\partial x_j}\left[\left(\nu+\frac{\nu_t}{\sigma_\gamma}\right)\frac{\partial\gamma}{\partial x_j}\right].\end{gathered}\tag{2}$$

Here $P_{\theta t}$ represents the production term for the momentum thickness Reynolds number; P_γ and E_γ are output and dispersal terms of the intermittency; $\sigma_{\theta t}$ and σ_γ are model constants.

Transition SST model (also known as $\gamma-\mathrm{R\tilde{e}}_{\theta t}$), equation (3):

$$\begin{gathered}\frac{\partial(\rho\gamma)}{\partial t}+\frac{\partial(\rho U_j\gamma)}{\partial x_j}=P_{\gamma1}-E_{\gamma1}+P_{\gamma2}-E_{\gamma2}+\frac{\partial}{\partial x_j}\left[\left(\mu+\frac{\mu_t}{\sigma_\gamma}\right)\frac{\partial\gamma}{\partial x_j}\right],\\ \frac{\partial(\rho\,\mathrm{R\tilde{e}}_{\theta t})}{\partial t}+\frac{\partial(\rho U_j\,\mathrm{R\tilde{e}}_{\theta t})}{\partial x_j}=P_{\theta t}+\frac{\partial}{\partial x_j}\left[\sigma_{\theta t}\left(\mu+\mu_t\right)\frac{\partial\mathrm{R\tilde{e}}_{\theta t}}{\partial x_j}\right].\end{gathered}\tag{3}$$

The given equations of the corresponding turbulence models are used to calculate the heat exchanger of direct flow type. For example, Figure 1 demonstrates a diagram of an externally insulated Thermal insulation straight tube-in-tube heat exchanger where two heat transfer fluids flow in parallel in the same direction. The cold coolant, oil, flows through the inner pipe, while the highly heated heat carrierin the outer pipe is water.

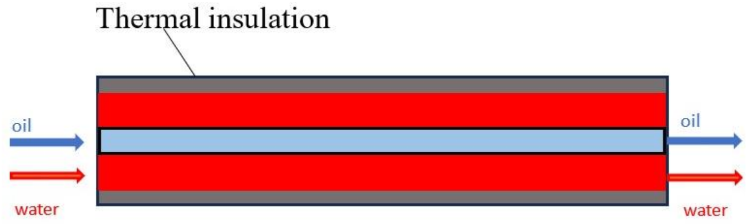

Figure 1. Schematic diagram of a heat exchanger of direct flow type (parallel flow)

When solving this problem, the following initial parameters for thermal calculation are used. The inner diameter of the pipe through which the cool heat carrier flows is 12 mm, and its outer diameter is 14 mm. The inner diameter of the pipe through which the highly heated heat carrier flows is 20 mm. Temperatures of cool and highly heated heat carriers in the inlet section are 303 K and 423 K. Mass flow rates of cool and highly heated heat carriers are equal to 0.3814 kg/s and 0.6386 kg/s (the velocity in the inlet section is assumed to be 4 m/s).

The results of calculations agree with the data of numerical modeling and with the results of distribution of the average mass temperature of oil and water (cold and hot coolants) along the length of the heat exchanger, obtained using the finite difference method and based on numerical modeling [11].

Results and Discussion

Figure 2 demonstrates comparative graphs of the change in the temperature of coolants along the tube of the heat exchanger for three models of turbulence for the direct flow of coolants. Here in the figure and further for all figures the following designations are introduced: 1 — $k-\omega$ SST model; 2 — $k-\varepsilon$ model; 3 — Transition SST model. The figure demonstrates that the temperature change curves of the coolants for all three models are alike, in that the temperature of the highly heated heat carrier declines while the temperature of the cool heat carrier arise throughout the tube.

It can also be noted that for all three turbulence models the temperature differences for both coolants are more noticeable and closer to the exit from the HE tubes. An analysis of the temperature change graphs also demonstrates that the graph of the heating temperature of the cold coolant (oil) along the tube for the $k-\varepsilon$ model is lower compared to the other two models, and the graph of the cooling temperature of the hot coolant is lower for the Transition SST model, while the intensity of oil heating is higher for the $k-\omega$ SST model.

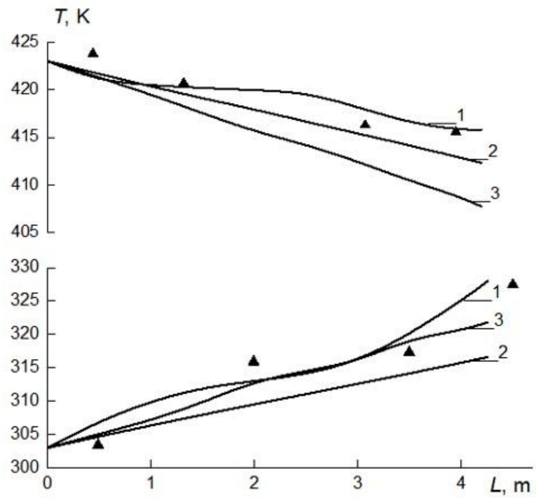

Figure 2. Variation of water (hot) and oil (cold) temperature along the length of the tube in parallel flow for all three models, the triangular icons correspond to the results of calculations using the LMTD method

This figure also demonstrates that for the $k-\varepsilon$ model, the temperature change for both coolants is linear along the length of the HE tubes.

The differences between the models are explained by sensitivity to viscosity profiles and turbulent energy distribution.

Figure 3 demonstrates the dissemination of the axial component of the oil velocity in the radial direction in the cross sections of the pipeline during straight flow for given turbulence models, namely the $k-\omega$ SST, $k-\varepsilon$ and Transition SST models. Velocity profiles are given at two cross sections of the HE tubes, namely at 1.5 m from the tube inlet and at the outlet, where these cross sections are shown in the figures. For all considered turbulence models, the velocity profiles have the form of logarithmic distribution. For the flow patterns of heat carriers in direct flow, the velocity profiles closest to the turbulent flow correspond to the $k-\omega$ SST and Transition SST models, which is natural, since the $k-\varepsilon$ turbulence model more accurately represents the movement outside the boundary layer, and heat exchange between the heat carriers occurs mainly in the boundary layer. Moreover, such profiles are pronounced in the cross-sections at the outlet of the tube.

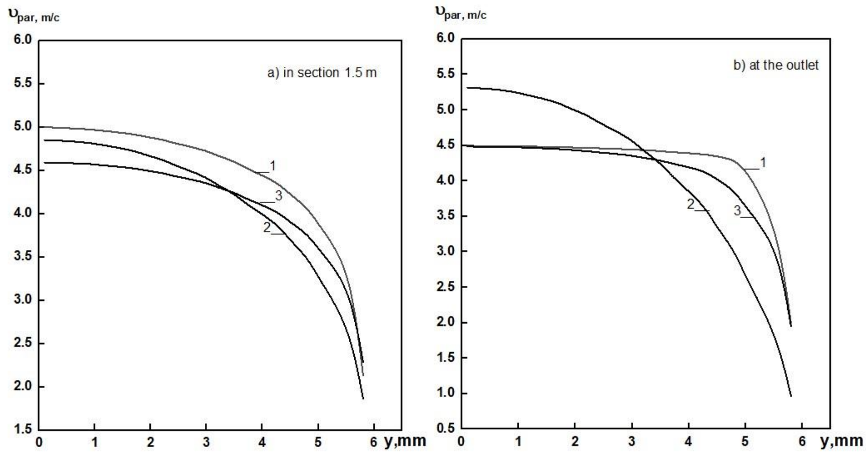

Figure 3. Dissemination of the axial component of oil velocity in different cross sections of the pipeline in the radial direction

The axial velocity component grows from center to wall depending on the model. The $k-\omega$ SST model gives smoother dissemination.

Figure 4*a* demonstrates a plot of the dependence of the Reynolds number Re on the tube length L in the case of straight flow for different turbulence models. It can be seen from this figure that the laminar-turbulent transition is clearly observed also in the straight stream within a distance x = 3–3.2 m for the case of $k-\omega$ SST model, and this transition for this model starts at numbers around Re = 2300 in the straight stream. For the other two turbulence models, this effect is weakly pronounced in the straight flow case.

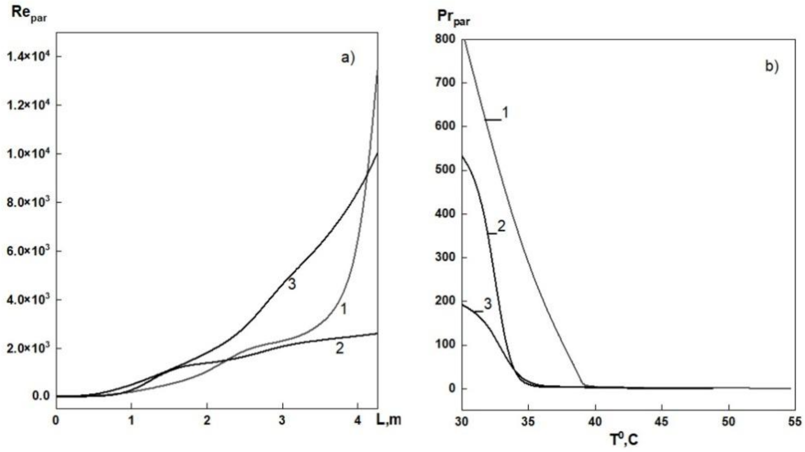

Figure 4. Distribution of Reynolds numbers for a smooth tube along the tube length (*a*) and dependence of the oil Prandtl number on temperature (*b*)

Figure 4*b* demonstrates the dependence of the Prandtl number for oil on temperature in cases of straight flow for turbulence models $k-\omega$ SST, $k-\varepsilon$, and Transition SST. From the figures it is clearly seen that for the scheme of straight flow of coolants, the movement of coolants at moderate temperatures (from 30 to 40 degrees Celsius) the value of Prandtl number has the highest value for the turbulence model $k-\omega$ SST and the lowest value for the Transition SST model, and for the model $k-\varepsilon$ values in between. Taking into account that the Prandtl number is defined as the ratio of the kinematic viscosity coefficient to the diffusivity of the medium, we can conclude that near the solid boundary of the tube the viscosity of the medium plays a significant role, which is expressed in the $k-\omega$ SST model.

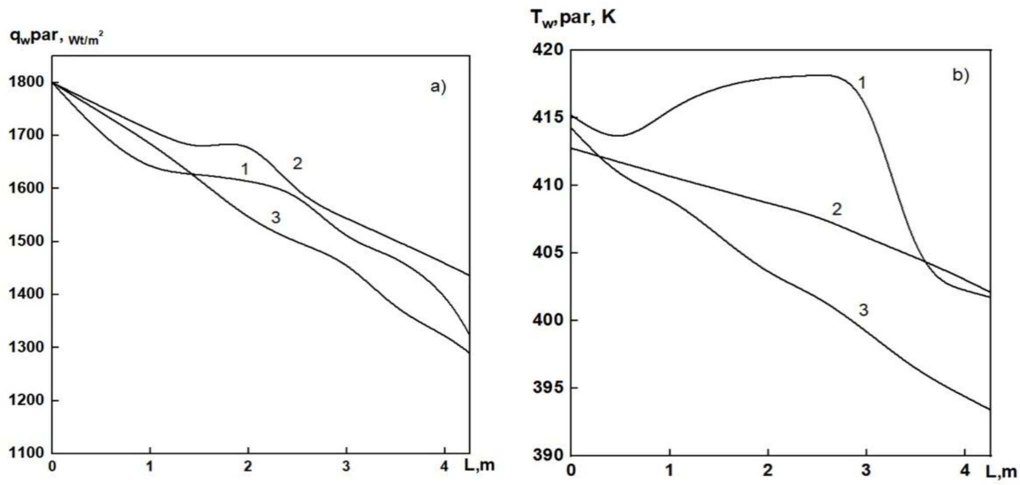

Figure 5. Variation of heat flux q_w along the length of the heat transfer wall (a) and wall temperature T_w along the length of the heat transfer wall on the oil side (b)

Figure 5*a* demonstrates the plots of heat flux q_w variation along the length of the heat transfer wall of the coolant motion for the three turbulence regimes. It can be seen from the plots that the behavior of the heat flux curves is identical for both schemes and for all turbulence models.

At high turbulence (curve 1) the wall temperature is higher along the entire length, which is due to improved heat transfer, while at lower turbulence (curve 3) the wall temperature is lower, indicating less efficient heat transfer. The temperature curves have a smoother and decreasing character along the length of the tube.

Figure 5*b* demonstrates modification in the temperature of the T_w wall along the length of the heat transfer wall from the oil side, where a laminar-turbulent transition is distinguished, this effect is not distinguished in the other two turbulence models.

In the case of strong dependence of viscosity on temperature as the coolant is heated, the flow regime changes from laminar to developed turbulent. In this case, using the local heat transfer coefficient α, the relationship for the local Nusselt number is valid: $\mathrm{Nu} = \alpha d_g / \lambda$.

Figure 6a demonstrates that the Nusselt number for the $k-\omega$ SST model is larger at the inlet of the HE tube; this can be explained by the fact that the Nusselt number characterizes the intensity of heat transfer due to convection, expressed through the heat transfer coefficient of the medium.

Figure 6b demonstrates the distribution of the heat transfer coefficient along the tube length for all three turbulence models considered. The heat transfer coefficient α was calculated by the known formula through the heat flux through the wall and the temperature difference between the liquid medium and the solid wall by the formula $\alpha = q_w / (T_w - T)$.

It can be seen from the figure that the laminar-turbulent transition for both flow patterns, i.e., also in the direct flow, is observed only for the $k-\omega$ SST model.

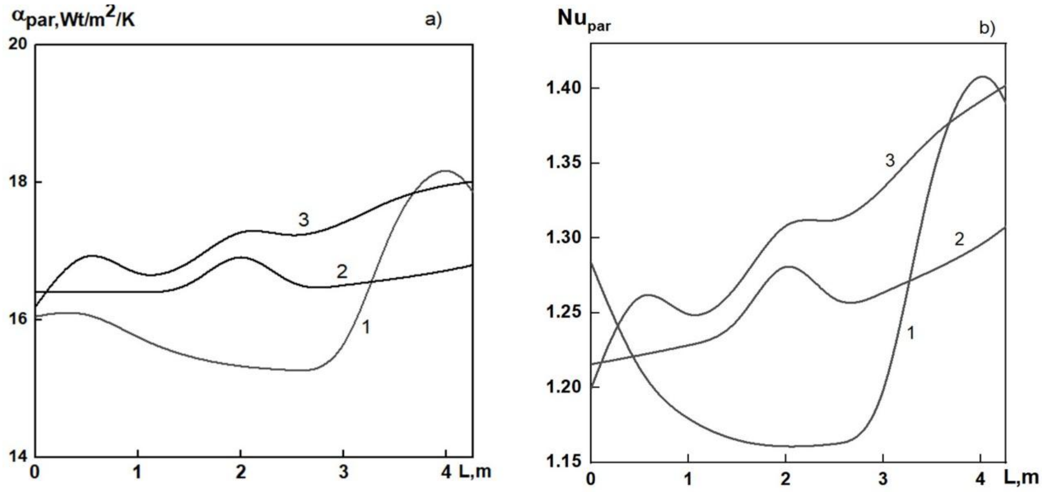

Figure 6. Dissemination of heat transfer coefficient along the length of the tube
and difference of number Nu along the length of the tube

From the given figure it is also possible to notice that in the region of the tube length $x = 3$ m, for both cases the laminar-turbulent transition of the oil flow regime is visible, while for other two turbulence regimes the change of Nu number along the tube length is more uniform. The results are compared with laminar regime (Poiseuille formula) and turbulent regime (Blasius and Nikuradze formulae).

Figure 7*a* demonstrates the curves of variation of overpressure values P_g along the length of the tube for the three turbulence regimes. Here, for all three turbulence modes, there is a drop in the overpressure (hence, and absolute) pressure along the entire length of the tube. At the exit of the tube, the overpressure approaches zero, i.e., the absolute pressure approaches the atmospheric pressure value. Here we also observe a significant increased pressure for the $k-\varepsilon$ turbulence model, which is probably explained by the failure to take into account the influence of the boundary layer in this turbulence model.

The pressure distribution along the tube steadily decreases as expected for steady flow. Figure 7b demonstrates the variation of the friction coefficient λ along the length of the tube for straight flow and counterflow for the three turbulence regimes.

The figure demonstrates that the values of the friction coefficient for the $k-\varepsilon$ turbulence are much higher than the corresponding values for the two turbulence regimes along the length of the tube, which is most likely a consequence of not taking into account the effect of the boundary layer on the tube wall.

At the same time, the values of λ for the $k-\varepsilon$ and Transition SST models in the graph lie higher in both shape and values. It should also be noted here that it is for the $k-\omega$ SST turbulence model that the laminar-turbulent transition is pronounced for both schemes and that occurs at a distance of 3–3.5 m from the beginning of the tube.

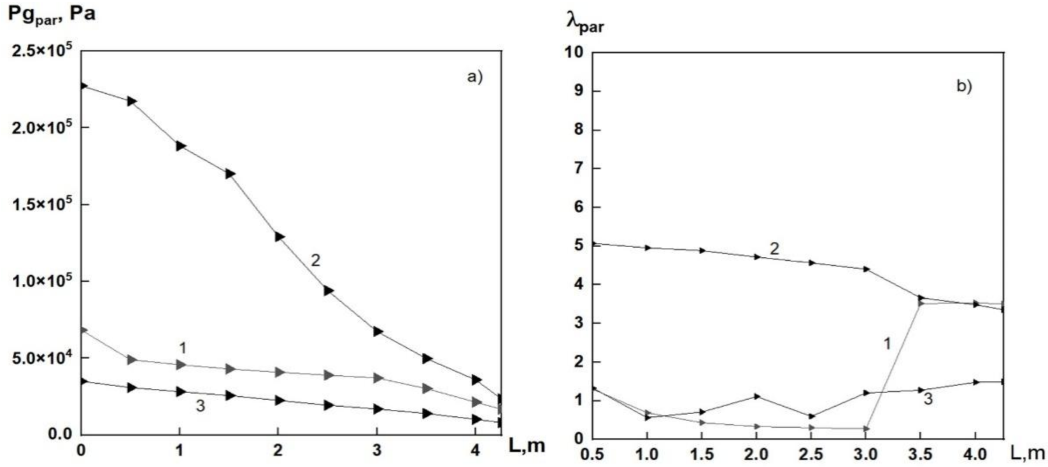

Figure 7. Variation of overpressure P_g and friction coefficient λ along the length of the tubing

Conclusion

Based on a numerical analysis of the heat exchanger of the type “tube-in-tube” using $k-\omega$ SST, $k-\varepsilon$ and Transition SST various turbulence models the following major results are obtained. For all turbulence models, a characteristic behavior of the temperature curves is observed: the temperature of the highly heated heat carrier declines while the temperature of the cool heat carrier rises along the length of the tube. The $k-\omega$ SST model demonstrates the greatest heating of the cool heat carrier, while the $k-\varepsilon$ model demonstrates a smoother and more linear behavior of the temperature profile. It follows from Figures 2 and 5*b* that the numerical values of the distribution of the mass average temperature of oil along the HE tube and its distribution along the tube surface are higher for the $k-\omega$ SST model, which indicates the effectiveness of using this model for numerical calculation.

The oil axial velocity profiles have a logarithmic shape for all models and are more pronounced for the $k-\omega$ SST and Transition SST models, especially in the outlet sections, indicating a more reliable modelling of turbulent processes near the wall. The $k-\varepsilon$ model reflects the boundary layer effect worse, which limits its applicability in problems with active heat transfer near the wall. The laminar-turbulent transition is most clearly recorded when using the $k-\omega$ SST model, in the range of 3–3.5 m from the tube inlet, which is confirmed by changes in the Reynolds number, heat transfer coefficient and friction coefficient.

For all models, the expected decrease in overpressure along the tube is observed. However, the $k-\varepsilon$ model demonstrates higher pressure values, probably due to insufficient consideration of boundary effects. Numerical values of heat flux through the tube wall appear to be higher for straight flow and heat transfer efficiency (in terms of Nusselt number) at the tube outlet. The Prandtl number for oil is maximized in the $k-\omega$ SST model, which is due to the largest contribution of the viscosity of the medium near the tube wall. This emphasizes the advantage of this model in modelling heat transfer with strong temperature dependence of viscosity.

Taking into account more accurate description of transient modes, correspondence of numerical simulation results to physical processes in the boundary layer and satisfactory representations of temperature and hydrodynamic profiles, the $k-\omega$ SST turbulence model can be considered as the most acceptable in calculations of heat exchangers with smooth tube surface in HE. These studies also emphasize the importance of a properly chosen mesh and the need to calibrate the models depending on specific heat transfer conditions or other processes.

References

1 Yogesh S.S. et al. Heat transfer and pressure drop characteristics of inclined elliptical fin tube heat exchanger of varying ellipticity ratio using CFD code / S.S. Yogesh, A.S. Selvaraj, D.K. Ravi et al. // International Journal of Heat and Mass Transfer. — 2018. — Vol. 119. — P. 26–39. https://doi.org/10.1016/j.ijheatmasstransfer.2017.11.094

2 Chen K. et al. Effects of non-uniform fin arrangement and size on the thermal response of avertical latent heat triple-tube heat exchanger / K. Chen, H. I. Mohammed, J. M. Mahdi et al. // Journal of Energy Storage. — 2022. — Vol. 45. — P. 103723. https://doi.org/10.1016/j.est.2021.103723

3 Osley W.G. CFD investigation of heat transfer and flow patterns in tube side laminar flow and the potential for enhancement / W.G. Osley, P. Droegemueller, P. Ellerby // Chemical Engineering Transactions. — 2013. — Vol. 35. — P. 997–1002. https://doi.org/10.3303/CET1335166

4 Karar O. et al. Experimental and numerical investigation on convective heat transfer in actively heated bundle-pipe / O. Karar, S. Emani, S.M. Gounder et al. // Engineering Applications of Computational Fluid Mechanics. — 2021. — Vol. 15, Issue 1. — P. 848–864. DOI: 10.1080/19942060.2021.1920466

5 Rana S. CFD approach for the enhancement of thermal energy storage in phase change material charged heat exchanger / S. Rana, M. Zunaid, R. Kumar // Case Studies in Thermal Engineering. — 2022. — Vol. 33. — P. 101921. https://doi.org/10.1016/j.csite.2022.101921

6 Allouche Y. et al. Validation of a CFD model for the simulation of heat transfer in a tubes-in-tank PCM storage unit / Y. Allouche, S. Varga, C. Bouden et al. // Renew. Energy. — 2016. — Vol. 89. — P. 371–379. https://doi.org/10.1016/j.renene.2015.12.038

7 Balaji D. CFD analysis of a pressure drop in a staggered tube bundle for a turbulent cross flow / D. Balaji, L. S. S. Prakash // Int. Adv. Res. J. Sci. Eng. Technol. — 2016. — Vol. 3. — P. 35–40. https://doi.org/10.17148/IARJSET.2016.3209

8 Czarnota T. Turbulent convection and thermal radiation in a cuboidal Rayleigh–Benard cell with conductive plates / T. Czarnota, C. Wagner // Int. J. Heat Fluid Flow. — 2016. — Vol. 57. — P. 150–172. https://doi.org/10.1016/j.ijheatfluidflow.2015.10.006

9 Mohanan A.K. Flow and heat transfer characteristics of a cross-flow heat exchanger with elliptical tubes / A.K. Mohanan, B.V. Prasad, S. Vengadesan // Heat Transf. Eng. — 2020. — Vol. 42. — P. 1846–1860. https://doi.org/10.1080/01457632.2020.1826742

10 Kurmanova D. et al. Modelling and Simulation of Heat Exchanger with Strong Dependence of Oil Viscosity on Temperature / D. Kurmanova, N. Jaichibekov, A. Karpenko, et al. // Fluids. — 2023. — Vol. 8, Issue 95. — P. 1–18. https://doi.org/10.3390/fluids8030095

11 Kurmanova D. Control of heat transfer characteristics in helicoidal heat exchangers with strong dependence of oil viscosity on temperature / D. Kurmanova, N. Jaichibekov, K. Volkov, A. Zhumanbayeva // 9th International Symposium on Advances in Computational Heat Transfer, CHT-24. — 2024. — P. 97–101. https://www.dl.begellhouse.com/references/1bb331655c289a0a,3ecc9d403d74976a, 52bf5fc425678078.

12 Kurmanova D.E. Numerical modeling and calculation of heat transfer between heat carriers in heat exchangers / D.E. Kurmanova, N.J. Jaichibekov, A.G. Karpenko, K.N. Volkov // Bulletin of the Karaganda University. Physics Series. — 2023. — № 1(109). — P. 59–70. DOI: https://doi.org/10.31489/2024ph2 /72-81

13 ANSYS Theory Guide / ANSYS, Inc. Southpointe. — Canonsburg, PA, 2019. — 988 p.

14 Лущик В.Г. Теплообменник «труба в трубе» с диффузорными каналами с газовыми и жидкими теплоносителями / В.Г. Лущик, А.И. Решмин, К.С. Егоров // Физико-химическая кинетика в газовой динамике. — 2024. — Том. 25, Вып. 4. — С. 1–21. http://chemphys.edu.ru/issues/2024-25-4/articles/1115/

А.С. Жұманбаева, Н.Ж. Жәйшібеков, Д.Е. Құрманова

Турбуленттік модельдердің жылу алмастырғыш аппараттарды есептеудегі жылу тасымалдағыштардың гидродинамикалық және жылулық параметрлеріне әсерін зерттеу

Мақалада *k*–ω SST, *k*–ε және transition SST турбуленттілігінің жартылай эмпирикалық модельдерін пайдалана отырып, тікелей ағындар схемасы үшін «құбырдағы құбыр» типті жылу алмастырғыштағы (ЖАА) суық (мұнай) және ыстық (су) жылу алмастырғыш арасында болатын жылу алмасу процестері зерттелді. Талдау нәтижелері көрсеткендей, түтіктің диаметрі өте аз жылу алмастырғышты есептеу кезінде түтіктегі шекаралық қабаттың әсерін ескере отырып, *k*–ω SST турбуленттілік моделі қолайлы болды. Бұл турбуленттілік моделі ламинарлы-турбулентті ауысуды айқынырақ көрсетеді, ол осы процестерде жүзеге асырылады, мұнда мұнайдың тұтқырлығы температураға өте тәуелді. Жылу алмасу процестерін сандық модельдеу және есептеу үшін ақырлы айырымды мен ақырлы көлем әдістері таңдалды. Есептеулер ANSYS Fluent бағдарламалық кешенін пайдалана отырып, есептеу гидродинамикасы (Computational Fluid Dynamics, CFD) құралдарының негізінде жүргізілді. Жылу алмастырғыштардың гидродинамикасын сандық модельдеу үшін ламинарлы — турбулентті ауысуды және модельдің *k*–ω SST теңдеулерін ескеретін gamma-Retheta турбуленттілік моделімен тұйықталған Рейнольдс бойынша орташа Навье-Стокс теңдеулері (RANS, Reynolds-averaged Navier — Stokes) қолданылды. Ұсынылған турбуленттілік моделі негізінде гидродинамикалық және жылу параметрлерінің таралуы, сондай-ақ ЖАА түтігінің ұзындығы бойынша процестің ұқсастық критерийлері (Re, Pr, Nu) алынды.

Кілт сөздер: жылу беру, сандық есептеу, жылу алмастырғыш, мұнай, гидродинамика, салқындатқыш сұйықтар, жылу ағыны, ламинарлы-турбулентті ауысу, үзіліссіздік, жылу алмасу қарқындылығы, тұтқырлық

А.С. Жуманбаева, Н.Ж. Джайчибеков, Д.Е. Курманова

Исследование влияния моделей турбулентности на гидродинамические и тепловые параметры теплоносителей в расчетах теплообменных аппаратов

В статье проведено исследование теплообменных процессов, происходящих между холодным (нефть) и горячим (вода) теплоносителями в теплообменном аппарате (ТОА) типа «труба в трубе» для схемы прямоток, с использованием полуэмпирических моделей турбулентности *k*–ω SST, *k*–ε и Transition SST. Анализ полученных результатов показал, что при расчете теплообменного аппарата с достаточно малым диаметром трубки более предпочтительной оказалась модель турбулентности *k*–ω SST, из-за учета влияния пограничного слоя в трубке. Данная модель турбулентности более выражено воспроизводит ламинарно-турбулентный переход, который осуществляется в данных процессах, где вязкость нефти сильно зависит от температуры. Для численного моделирования и расчета теплообменных процессов были выбраны методы конечных разностей и конечных объемов. Расчеты проводились на основе средств вычислительной гидродинамики (Computational Fluid Dynamics, CFD), с использованием программного комплекса Ansys Fluent. Для численного моделирования гидродинамики теплоносителей применялись осредненные по Рейнольдсу уравнения Навье-Стокса (RANS, Reynolds-averaged Navier-Stokes), замкнутые при помощи модели турбулентности gamma-Retheta, учитывающей ламинарно-турбулентный переход и уравнения *k*–ω SST модели. На основе предложенной модели турбулентности получены распределения гидродинамических и тепловых параметров, а также критериев подобия (Re, Pr, Nu) процесса по длине трубки ТОА.

Ключевые слова: теплопередача, численный расчет, теплообменник, нефть, гидродинамика, охлаждающие жидкости, тепловой поток, ламинарно-турбулентный переход, перемежаемость, интенсивность теплообмена, вязкость

References

1 Yogesh, S.S., Selvaraj, A.S., Ravi, D.K., & Rajagopal, T.K.R. (2018). Heat transfer and pressure drop characteristics of inclined elliptical fin tube heat exchanger of varying ellipticity ratio using CFD code. *International Journal of Heat and Mass Transfer, 119*, 26–39. https://doi.org/10.1016/j.ijheatmasstransfer.2017.11.094

2 Chen, K., Mohammed, H.I., Mahdi, J.M., Rahbari, A., Cairns, A., & Talebizadehsardari, P. (2022). Effects of non-uniform fin arrangement and size on the thermal response of a vertical latent heat triple-tube heat exchanger. *Journal of Energy Storage, 45*. 103723. https://doi.org/10.1016/j.est.2021.103723

3 Osley, W.G., Droegemueller, P., & Ellerby, P. (2013). CFD investigation of heat transfer and flow patterns in tube side laminar flow and the potential for enhancement. *Chemical Engineering Transactions, 35*, 997–1002. DOI: 10.3303/CET1335166

4 Karar, O., Emani, S., Gounder, S.M., Myo Thant, M.M., Mukhtar, H., Sharifpur, M., & Sadeghzadeh, M. (2021). Experimental and numerical investigation on convective heat transfer in actively heated bundle-pipe. *Engineering Applications of Computational Fluid Mechanics, 15*(1), 848–864. DOI: 10.1080/19942060.2021.1920466

5 Rana, S., Zunaid, M., & Kumar, R. (2022). CFD approach for the enhancement of thermal energy storage in phase change material charged heat exchanger. *Case Studies in Thermal Engineering, 33*, 101921. https://doi.org/10.1016/j.csite.2022.101921

6 Allouche, Y., Varga, S., Bouden, C., & Oliveira, A.C. (2016). Validation of a CFD model for the simulation of heat transfer in a tubes-in-tank PCM storage unit. *Renewable Energy, 89*, 371–379. https://doi.org/10.1016/j.renene.2015.12.038

7 Balaji, D., & Prakash, L.S.S. (2016). CFD analysis of a pressure drop in a staggered tube bundle for a turbulent cross flow. *International Advanced Research Journal in Science, Engineering and Technology, 3*(2), 35–40. https://doi.org/10.17148/IARJSET.2016.3209

8 Czarnota, T., & Wagner, C. (2016). Turbulent convection and thermal radiation in a cuboidal Rayleigh-Binard cell with conductive plates. *International Journal of Heat and Fluid Flow, 57*, 150–172. https://doi.org/10.1016/j.ijheatfluidflow.2015.10.006

9 Mohanan, A.K., Prasad, B.V., & Vengadesan, S. (2021). Flow and heat transfer characteristics of a cross-flow heat exchanger with elliptical tubes. *Heat Transfer Engineering, 42*(21), 1846–1860. https://doi.org/10.1080/01457632.2020.1826742

10 Kurmanova, D., Jaichibekov, N., Karpenko, A., & Volkov, K. (2023). Modelling and Simulation of Heat Exchanger with Strong Dependence of Oil Viscosity on Temperature. *Fluids, 8*(95), 1–18. https://doi.org/10.3390/fluids8030095

11 Kurmanova, D., Jaichibekov, N., Volkov, K., & Zhumanbayeva, A. (2024). Control of heat transfer characteristics in helicoidal heat exchangers with strong dependence of oil viscosity on temperature. *9th International Symposium on Advances in Computational Heat Transfer*, CHT-24, 97–101. https://www.dl.begellhouse.com/references/1bb331655c289a0a,3ecc9d403d74976a,52bf5fc425678078.

12 Kurmanova, D.E., Jaichibekov, N.J., Karpenko, A.G., & Volkov, K.N. (2023). Numerical modeling and calculation of heat transfer between heat carriers in heat exchangers. *Bulletin of the University of Karaganda–Physics*, 1(109), 59–70. DOI: https://doi.org/10.31489/2023ph1/59-70

13 ANSYS Fluent Theory Guide. (2019). ANSYS, Inc. Southpointe. — Canonsburg, PA, 988.

14 Lushchik, V.G., Reshmin, A.I., & Egorov, K.S. (2024). Teploobmennik «truba v trube» s diffuzornymi kanalami s gazovymi i zhidkimi teplonositeliami [Double-Pipe Heat Exchanger with Diffuser Channels with Gas and Liquid Coolants]. *Fiziko-khimicheskaia kinetika v gazovoi dinamike — Physical-Chemical Kinetics in Gas Dynamics, 25*(4), 1–21 [in Russian].

Information about the authors

Zhumanbayeva, Aizhan — Doctoral student, Department of Mechanics, L.N. Gumilyov Eurasian National University, Astana, Kazakhstan; e-mail: aizhanzhumanbayeva347@gmail.com; ORCID ID: https://orcid.org/0009-0007-2725-3672

Jaichibekov, Nurbolat (*contact person*) — Doctor of Physical and Mathematical Sciences, Professor, Department of Mechanics, L.N. Gumilyov Eurasian National University, Astana, Kazakhstan; e-mail: jaich@mail.ru; ORCID ID: https://orcid.org/0000-0002-3053-8288

Kurmanova, Dinara — PhD, Department of Mechanics, L.N. Gumilyov Eurasian National University, Astana, Kazakhstan; e-mail: dikonya89_29@mail.ru; ORCID ID: https://orcid.org/0009 0009-9787-7426